Importance of Coriolis Coupling in Isotopic Branching in (He, HD^+) Collisions

Ashwani Kumar Tiwari,[†] Sujitha Kolakkandy,[†] and N. Sathyamurthy*[,†,‡]

Department of Chemistry, Indian Institute of Technology Kanpur, Kanpur 208016, India, Indian Institute of Science Education and Research Mohali, MGSIPAP Complex, Sector 26, Chandigarh 160019, India

Received: May 27, 2009; Revised Manuscript Received: July 10, 2009

A three-dimensional time-dependent quantum mechanical wave packet approach is used to calculate the reaction probability (P^R) and integral reaction cross section values for both channels of the reaction He + $HD^+(v = 1; j = 0) \rightarrow$ HeH $(D)^+$ + D (H) over a range of translational energy (E_{trans}) on the McLaughlin−Thompson−Joseph−Sathyamurthy potential energy surface including the Coriolis coupling (CC) term in the Hamiltonian. The reaction probability plots as a function of translational energy for different J values exhibit several oscillations, which are characteristic of the system. The σ^R values obtained by including CC and not including it are nearly the same over the range of E_{trans} investigated for the HeD^+ channel. For the HeH^+ channel, on the other hand, σ^R values obtained from CC calculations are significantly smaller than those obtained from coupled state calculations. These results are compared with the available experimental results. The computed branching ratios ($\Gamma_\sigma = \sigma^R$ $(HeH^+)/\sigma^R$ (HeD^+)) are also compared with the available experimental results.

1. Introduction

To date, exact three-dimensional, time-dependent quantum mechanical (TDQM) calculations including Coriolis coupling (CC) are available only for a few triatomic systems. Meijer and Goldfield[1] carried out a TDQM wave packet study including Coriolis coupling for the H + $O_2 \rightarrow$ OH + O reaction on parallel computers. They performed calculations for total angular momentum $J = 1$, $J = 2$, $J = 5$, and $J = 10$ under centrifugal sudden (CS) approximation as well as including Coriolis coupling using two different embeddings for the body fixed coordinate system to investigate the importance of Coriolis coupling for this reactive system. When they considered the H−O_2 center-of-mass separation as the z axis of the coordinate system, they found poor agreement between the results from CS and CC calculations for $J > 2$. When they considered the O_2 bond as the z axis, they found good agreement between the CC and CS results at low J. For higher J values, the agreement became progressively worse, especially at higher energies. In subsequent studies, they computed J-converged integral reaction cross section (σ^R) values by including the CC term.[2] Recently, Padmanaban and Mahapatra[3] have carried out TDQM studies including CC terms for the H + HLi reaction. They considered coupling between the neighboring K states up to $K_{max} = 8$. They found that resonance oscillations in the reaction probability versus energy curve tended to become broader on inclusion of the CC term. The σ^R values obtained by including the CC terms were generally lower than those obtained using the CS approximation. To date, all the TDQM studies on the He + H_2^+ $\rightarrow$ HeH^+ + H reaction except that of Chu et al.[4] were under CS approximation. The most recent TDQM study on the system under CS approximation by Panda and Sathyamurthy[5] using the Palmieri et al. potential energy surface (PES)[6] confirmed the vibrational enhancement of the reaction cross section and also the survival of reactive scattering resonances in the calculated reaction probability with J averaging. Recently, Tang et al.[7] measured the σ^R values for the reaction for different vibrational (v) and rotational (j) states of H_2^+ over a range of E_{trans}. There were some quantitative discrepancies between the CS results and the experimental results. It was surmised that such discrepancies arose from neglecting the CC term and also from the calculations' being restricted to the rotational ground state ($j = 0$). The predicted reactive scattering resonances by the quantum scattering calculations of Panda and Sathyamurthy for the system have not yet been confirmed by experiments. To examine the importance of Coriolis coupling, Chu et al.[4] carried out 3D TDQM studies by including the CC term in the Hamiltonian on the Palmieri el al. PES. They compared their CC cross section values with the CS cross section values of Panda and Sathyamurthy and with the experimental initial state-selected cross section values reported by Tang et al. It was found that neglecting the CC could significantly alter the value of the computed reaction cross section and its dependence on E_{trans}. The excitation function for $v = 2$ obtained in their CC calculations revealed a sharp rise at the reaction threshold ($E_{trans} = 0.265$ eV), followed by a decline at higher collision energies. Excitation functions for $v = 4$ and 6 exhibited a general declining trend, but a kink was observed at low collision energies for $v = 4$. In contrast to the reaction probability versus E_{trans} plots, which revealed sharp resonances at low collision energies, the calculated reaction cross section versus E_{trans} plots showed only slight oscillations, indicating little chance of survival of the resonances on J and K averaging. Their CC results were in better agreement with the experimental results than the CS results of Panda and Sathyamurthy. The large differences between the CS and the CC results of reaction probability and integral cross section values suggested that Coriolis coupling plays an important role in the dynamics of this system. Here, one must point out that Palmieri et al.[6] had carried out time-independent quantum calculations using hyperspherical coordinates and including Coriolis coupling for $K_{max} = 6$ for the (He, H_2^+) reaction.

The TDQM studies on (He, HD^+) reported by us in refs 8 and 9 were carried out under CS approximation. In view of the findings by Chu et al., it became necessary to investigate the importance of including the CC term in the Hamiltonian in the dynamics of (He, HD^+) collisions. Therefore, a detailed

* Corresponding author. E-mail: nsath@iitk.ac.in.
† Indian Institute of Technology Kanpur.
‡ Indian Institute of Science Education and Research Mohali.

10.1021/jp9049523 CCC: $40.75
Published on Web 07/30/2009

TABLE 1: Grid Parameters and Initial Condition Details for $J \leq 13$[a]

parameters	values	descriptions
N_R	128	no. grid points in R
$(R_{min}, R_{max})/a_0$	(1.50, 16.74)	range of R values
N_r	80	no. grid points in r
$(r_{min}, r_{max})/a_0$	(1.00, 12.06)	range of r values
N_γ	54	no. grid points in γ
Δt/fs	0.2419	time step used in propagation
T/ps	1.2	propagation time
R_0/a_0	12.0	center of the initial wave packet
δ/a_0	0.25	Gaussian width parameter
r_s/a_0	7.0	position of the analysis surface

[a] See text for $J > 13$.

TDQM study of (He, HD^+) dynamics including the CC term was undertaken on the MTJS PES.[10] Details of the methodology are given in Section 2, and the results are presented and discussed in Section 3. Summary and conclusions follow in Section 4.

2. Methodology

The TDQM methodology[11,12] used involves solving the time-dependent Schrödinger equation in reactant channel Jacobi coordinates on a three-dimensional grid. For a triatomic system, the Hamiltonian operator in (R, r, γ) space is given as[13]

$$\mathbf{H} = -\frac{\hbar^2}{2\mu_R}\frac{\partial^2}{\partial R^2} - \frac{\hbar^2}{2\mu_r}\frac{\partial^2}{\partial r^2} + \frac{(\mathbf{J}-\mathbf{j})^2}{2\mu_R R^2} + \frac{\mathbf{j}^2}{2\mu_r r^2} + V(R, r, \gamma) \quad (1)$$

where μ_R is the reduced mass of He relative to the center-of-mass of HD^+ and μ_r is the reduced mass of HD^+. R is the center of mass separation between He and HD^+, r is the separation between H and D, and γ is the angle between R and r. $\mathbf{J}$ is the total angular momentum operator, and $\mathbf{j}$ is the rotational angular momentum operator for the diatomic species. $V(R, r, \gamma)$ is the interaction potential.

The initial wave packet at time $t = 0$ was chosen as

$$\psi(R, r, \gamma, t = 0) = G_{k_0}(R)\, \varphi_{vj}(r)\, P_{jK}(\cos\gamma) \quad (2)$$

where

$$G_{k_0} = \left(\frac{1}{\pi\delta^2}\right)^{1/4} \exp\{-(R - R_0)^2/2\delta^2\} \exp(-ik_0R) \quad (3)$$

with R_0 and k_0 referring to the center of the wave packet in position and momentum space, respectively. δ is the width parameter for the wave packet, K is the projection of J on the body fixed z axis (taken along R) and $P_{jK}(\cos\gamma)$ represents the associated Legendre polynomials.

The diatomic rovibrational eigenfunctions $\phi_{vj}(r)$ for HD^+ were computed by means of the Fourier grid Hamiltonian approach.[14]

The split-operator method[15] was used to propagate the wave packet in time. The fast Fourier transform (FFT) method[16] was used to solve the radial part of the Schrödinger equation, and the discrete variable representation (DVR)[17−19] was used for the angular part. The time-dependent Schrödinger equation including Coriolis coupling was solved, and the wave packet was propagated for 1.20−1.70 ps. In the CS approximation, K is a good quantum number (K is conserved), and therefore, calculations are carried out by treating K as a fixed parameter, whereas in the CC calculations, adjacent K states are coupled to each other (i.e., K with $K \pm 1$). Therefore, in the CC calculations, in addition to the three Jacobi coordinates, K also adds to the overall dimensionality. Full calculations were done for $J \leq 10$. For $10 < J \leq 27$, K_{max} was set to 10 and for $J > 27$, $K_{max} = 5$. This was necessary to keep the computation manageable.

Having computed $\psi(R, r, \gamma, t)$ at time t, the energy resolved reaction probability $p_{vj}^{JK}(E)$ was calculated as[20]

$$P_{vj}^{JK}(E) = \frac{\hbar}{\mu_r} Im \times \left[\int_0^\infty dR \int_0^\pi d\gamma \sin\gamma \psi^*(R, r, \gamma, E) \frac{d}{dr} \psi(R, r, \gamma, E)\right]_{r=r_s} \quad (4)$$

where the energy-dependent wave function $\psi(R, r, \gamma, E)$ was obtained by Fourier transforming the time-dependent wave packet $\psi(R, r, \gamma, t)$.

Distance criteria have been used to assign the flux to each channel. If r_{HeH^+} is less than r_{HeD^+}, the flux is assigned to the HeH^+ channel. Otherwise, it is assigned to HeD^+. For computing reaction probabilities corresponding to HeH^+ and HeD^+ channels, r_s has been taken to be sufficiently large and away from the interaction region. Depending upon the values of r_{HeH^+} and r_{HeD^+}, the flux was integrated into either of the two channels. It was verified that the sum of the reaction probabilities obtained from individual product channels and the total reaction probability obtained directly from the energy-resolved flux out of reactant channel were equal.

The J-dependent initial state-selected partial reaction cross section σ_{vj}^J was determined as

$$\sigma_{vj}^J(E_{trans}) = \frac{1}{(2j+1)}\left[P_{vj}^{JK=0}(E_{trans}) + 2\sum_{K=1}^{K_{max}} P_{vj}^{JK}(E_{trans})\right] \quad (5)$$

The initial state-selected total reaction cross section $\sigma_{vj}(E_{trans})$ was then obtained by summing over the partial reaction cross section values for all the partial waves:

$$\sigma_{vj}(E_{trans}) = \frac{\pi}{k_{vj}^2}\sum_{J=0}^{J_{max}} (2J+1)\, \sigma_{vj}^J(E_{trans}) \quad (6)$$

The parameters used in the calculations for $J \leq 13$ are given in Table 1. For $J > 13$, R_o was increased by one atomic unit for each unit increase in J. Correspondingly the time duration of propagation of the wave packet is also increased. Further details of the methodology can be seen in an earlier publication.[21]

3. Results and Discussion

Computed P^R values for both the product channels, HeH^+ and HeD^+, are plotted as a function of J and E_{trans} for $v = 1$, $j = 0$ in Figures 1 ($K = 0$, 1 and 2) and 2 ($K = 3$, 4, and 5). There are a large number of oscillations in $P^R(E_{trans})$ for both the channels indicating the importance of resonances in the dynamics of (He, HD^+) collisions. It is clear that there is an overall increase in P^R values with an increase in E_{trans} for

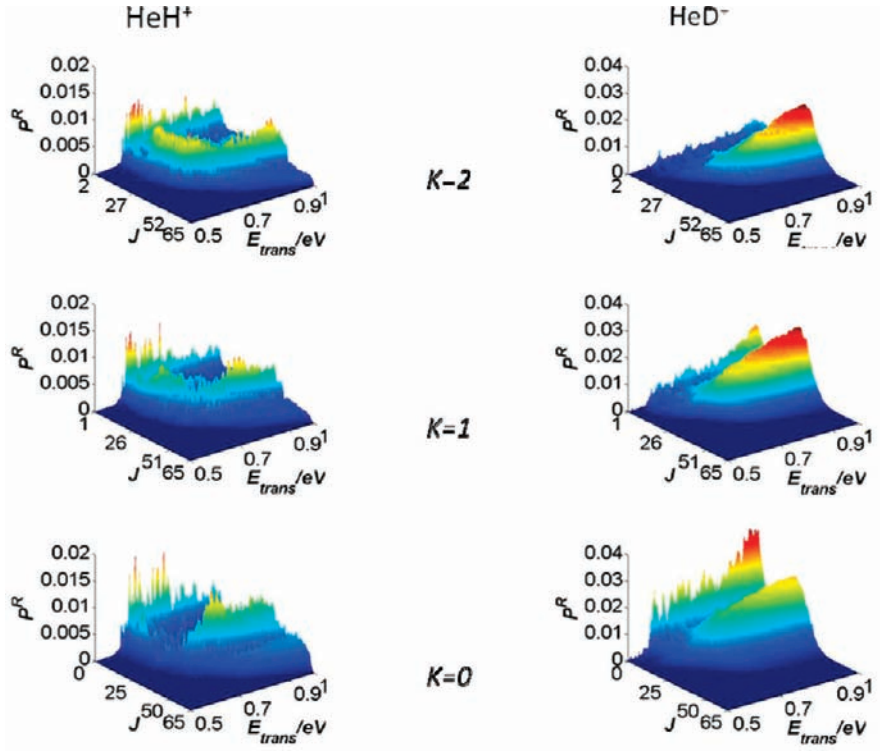

Figure 1. Reaction probability for HeH^+ and HeD^+ formation as a function of J and E_{trans} for $v = 1$, $j = 0$ of HD^+ for $K = 0$, 1, and 2.

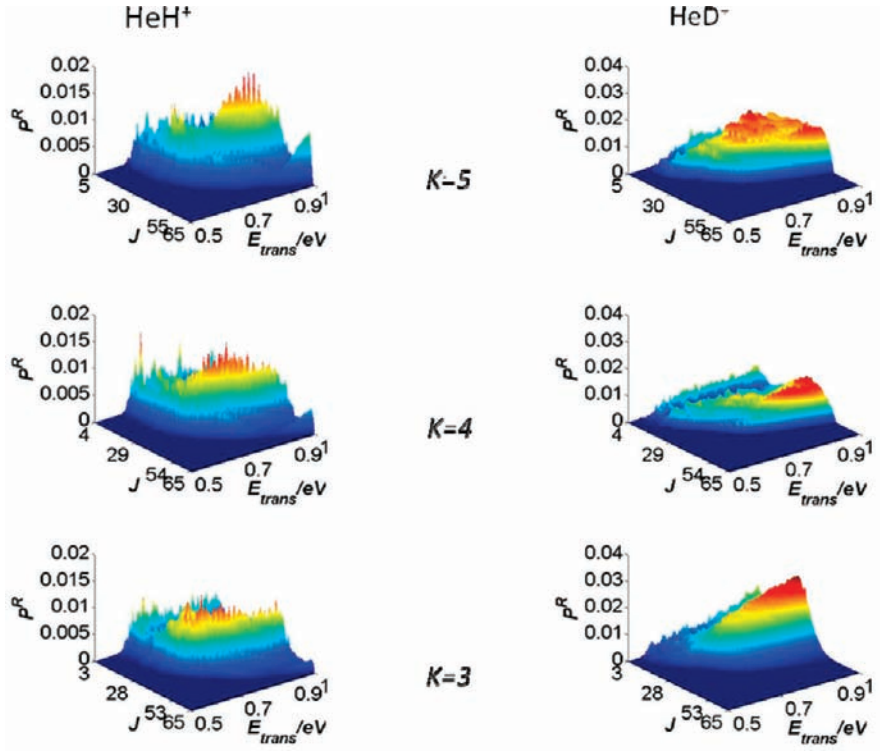

Figure 2. Same as in Figure 1 for $K = 3$, 4, and 5.

both of the channels for all the K values. The P^R values for all the K states decrease initially with an increase in J and then increase with an increase in J and again start decreasing with an increase in J. The decrease in P^R value with increase in J is understandable because the effective barrier for the reaction increases with increase in J. The reason for the increase in P^R with increase in J for intermediate values of J is not clear. Chu et al.[4] also found that for $He + H_2^+$ reactions, the P^R values obtained from their CC calculations increased with an increase in J up to $J = 20$ and then started decreasing on a further increase in J. One could explain the increase in $P^R(J)$ in terms of the Coriolis force. With an increase in J, the Coriolis force would become increasingly important, and the bond would be stretched, with the effect that the molecule would behave as if it is vibrationally excited. With an increase in J beyond 20, probably the

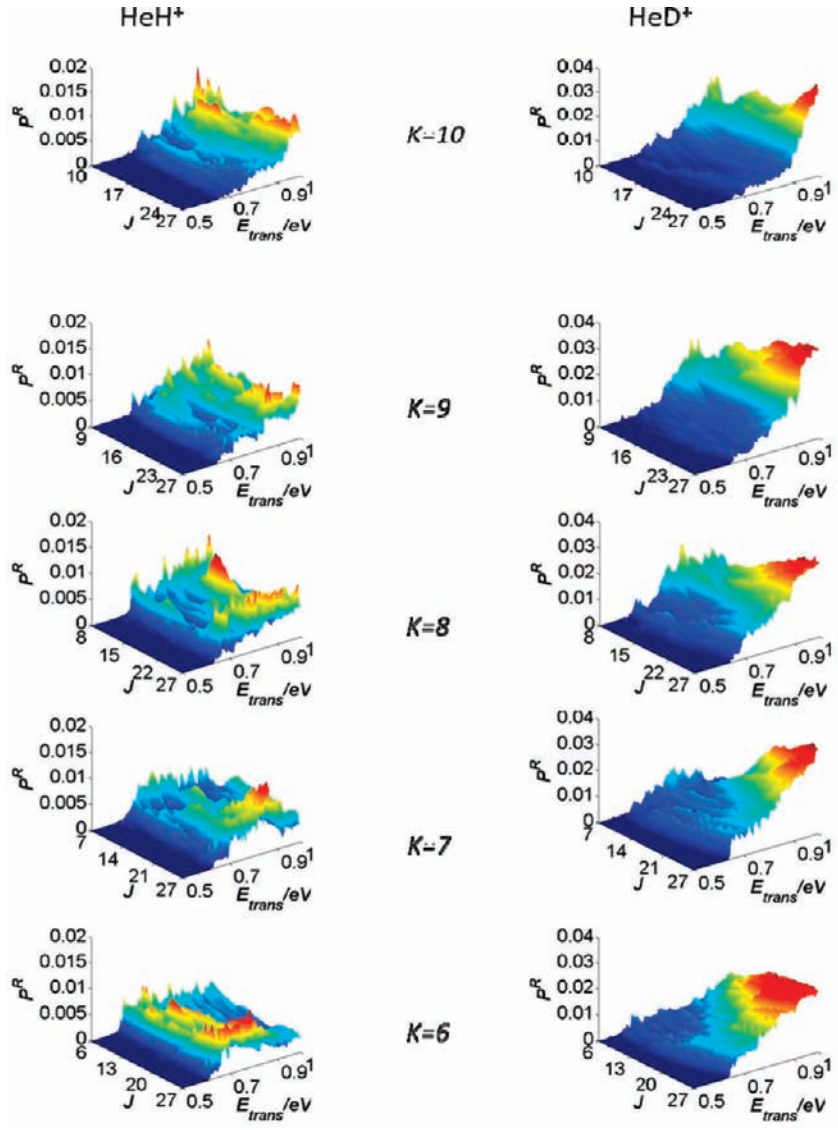

Figure 3. Same as in Figures 1 and 2 but for $K = 6$, 7, 8, 9, and 10.

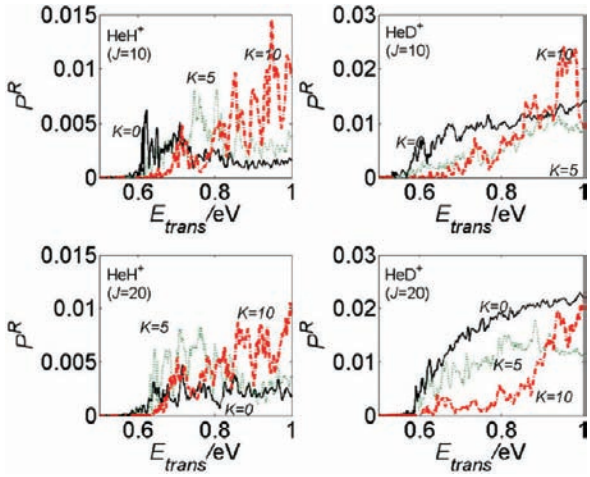

Figure 4. Reaction probability for $K = 0$, 5, and 10 for $J = 10$ and 20 as a function of E_{trans}.

centrifugal barrier becomes the dominant factor. The maximum value of J (J_{max}) for which P^R becomes zero is larger for the HeH$^+$ channel than for the HeD$^+$. This was also found in our CS calculations.[8,9]

The reaction probability is plotted as a function of J (≤ 27) and E_{trans} for $K = 6-10$ in Figure 3. This restriction became necessary because of the limited computational facility available with us currently. These plots are similar to those of Figures 1 and 2. P^R decreases with an increase in K at lower translational energies. For illustrative purposes, the plots of $P^R(E_{trans})$ for both HeH$^+$ and HeD$^+$ channels for $J = 10$ and $J = 20$ are given in Figure 4. Clearly, the value of P^R is strongly dependent on the value of K. The sensitivity becomes larger at larger E_{trans}. Interestingly, the dependence of P^R on K is different for the two channels. For HeH$^+$ formation, P^R generally is larger for larger K within the energy range considered here. For HeD$^+$, on the other hand, P^R decreases with an increase in K from 0 to 5, and the trend is reversed on increasing K to 10 at higher E_{trans}.

To examine the sensitivity of the dynamics to K at $E_{trans} = 1.0$ eV, the partial reaction cross section $[(2J + 1)P^R]$ values are plotted as a function of J for different values of K in Figure 5. It is clear that the plot of $[(2J + 1)P^R]$ as a function of J for the HeH$^+$ channel shows more oscillatory behavior than that for the HeD$^+$ channel. In CS calculations, it was found that the partial cross section for HeH$^+$ formation decreased with an increase in K, whereas it increased with an increase in K for

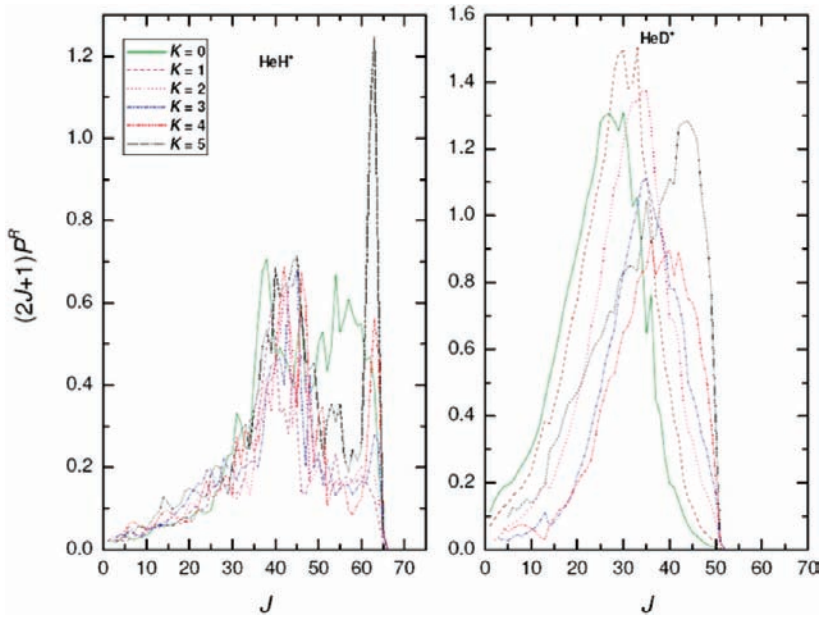

Figure 5. Partial reaction cross section for the formation of HeH^+ and HeD^+ as a function of J for different K values at $E_{trans} = 1.0$ eV for $v = 1$, $j = 0$ of HD^+.

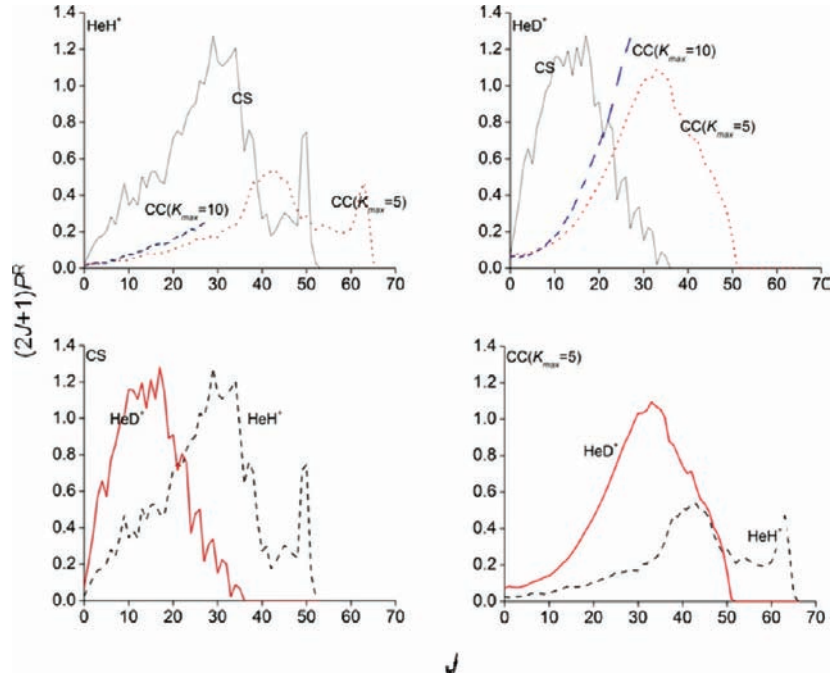

Figure 6. Plot of K-weighted $(2J + 1)P^R$ values for the formation of HeH^+ and HeD^+ as a function of J at $E_{trans} = 1.0$ eV for $v = 1$, $j = 0$ of HD^+ compared with the results obtained using the CS approximation.

the HeD^+ channel for all the J values. But in CC calculations, the dependence of the partial cross section values on K changes with a change in J. The K-weighted $[(2J + 1)P^R]$ values obtained from CC calculations at $E_{trans} = 1.0$ eV are plotted as a function of J in Figure 6. For comparison, $[(2J + 1)P^R]$ values obtained from CS calculations are also plotted in the same figure. The results for $J \leq 27$, with $K_{max} = 10$ are also included. The CC results show convergence at larger J values than the CS results for both the exchange channels. The inclusion of larger K values in CC calculations shows a slight increase in the partial cross section for both the channels. This must be due to a larger contribution from the larger K values at $E_{trans} = 1.0$ eV. A comparison of the CS and CC results for $K = 0$ in Figure 7 emphasizes the importance of CC.

It is clear that the $[(2J + 1)P^R]$ values for both the channels obtained from CS calculations are larger than those obtained from CC calculations at low J values, whereas at high J values, the trend gets reversed. But both the CC and CS calculations show that HeD^+ is preferred over HeH^+ at low J values, whereas at high J values, HeH^+ is preferred over HeD^+. Therefore, the preferential scattering of one isotopomer over another (HeH^+ is preferred over HeD^+ in the forward direction and HeD^+ is preferred over HeH^+ in the backward direction) reported in refs 8, 9, and 22 under CS approximation is also valid in CC calculation.

The computed σ^R values for $v = 1$, $j = 0$ from CC and CS calculations are plotted as a function of E_{trans} in Figure 8, along with the experimental results for $v = 1$ of HD^+.[23,24] It is

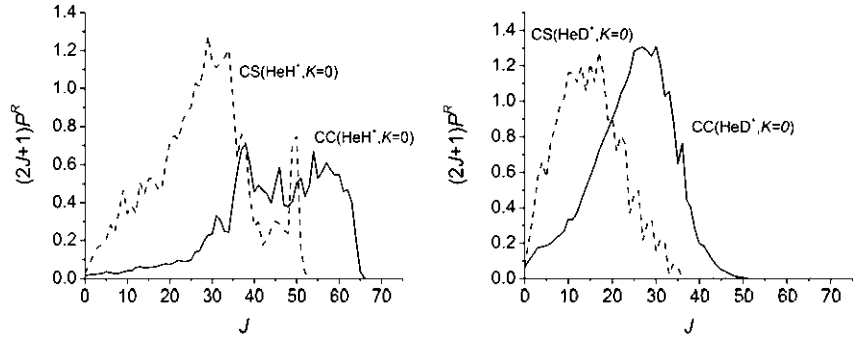

Figure 7. Plot of partial reaction cross section values for $K = 0$ from CS and CC calculations.

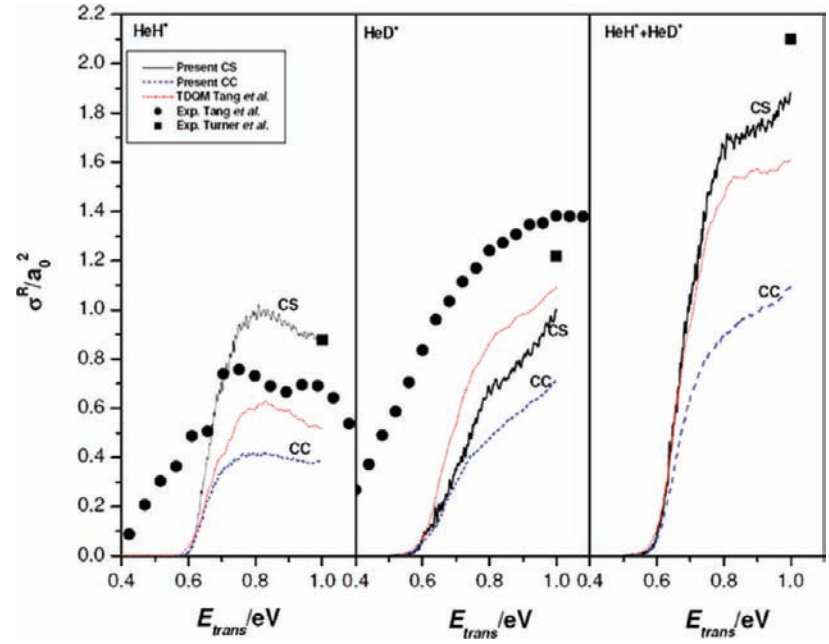

Figure 8. Plot of integral reaction cross section as a function of E_{trans} for the formation of (a) HeH^+, (b) HeD^+, and (c) both HeH^+ and HeD^+ for $v = 1, j = 0$ of HD^+ as obtained from the present study, as compared with the earlier results obtained using CS approximation and the experimental results.

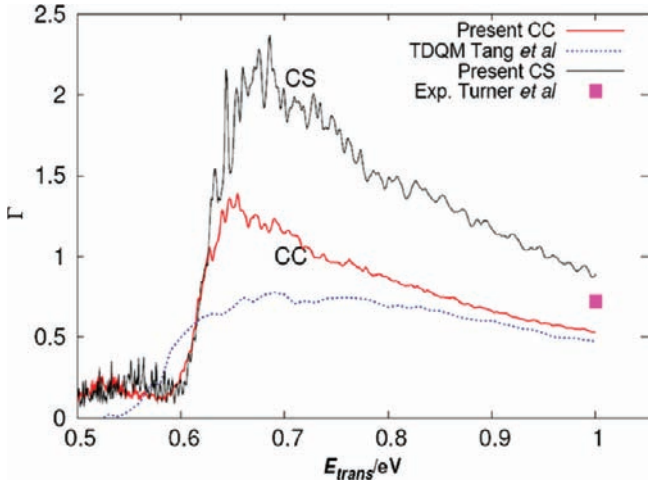

Figure 9. Plot of isotopic branching ratio as a function of E_{trans} for $v = 1, j = 0$ of HD^+ as obtained from the present study compared with the earlier CS results and the experimental results.

important to point out that the experimental results of Turner et al. are not *j*-selected, and those by Tang et al. are for $j = 1$. The TDQM results for $v = 1, j = 1$ of HD^+ on the Palmieri et al. PES by Tang et al.[25] is also plotted in the same figure. It is clear that the σ^R values obtained from CC and CS calculations are comparable for HeD^+ over the entire range of E_{trans}. Computed σ^R values for HeD^+ are smaller than the experimental values reported by Tang et al. over the entire E_{trans} range. For the HeH^+ channel, CC calculations give much smaller σ^R values than the CS calculations. In addition, oscillations in the excitation function plot nearly disappear in CC calculations. Interestingly, the experimental value of σ^R for the formation of HeH^+ as obtained from Turner et al. agrees with the CS result. Experimental σ^R values by Tang et al. are larger than both CC and CS cross section values in the threshold region. At higher E_{trans} values, experimental σ^R values are smaller than the CS cross section values and larger than the CC cross section values. The computed isotopic branching ratio [$\Gamma_\sigma = \sigma^R$ (HeH^+)/σ^R (HeD^+)] is plotted as a function of E_{trans} in Figure 9, along with the experimental value. Clearly, Γ_σ values obtained from CC calculations are smaller than those obtained from CS calculations over the entire E_{trans} range. The experimental Γ_σ value at $E_{trans} = 1.0$ eV by Turner et al. is slightly lower than the CS value and slightly larger than the CC value.

4. Summary and Conclusion

Initial state-selected reaction probabilities and integral reaction cross section values for the reaction He + HD^+ ($v = 1, j = 0$) → HeH(D)$^+$ + D(H) have been computed using a time-dependent quantum mechanical wave packet approach on the

MTJS potential energy surface. The integral reaction cross section values for HeD^+ obtained from CC and CS calculations are nearly the same over the entire E_{trans} range. For the HeH^+ channel, the σ^R values obtained by including CC are lower than the σ^R values obtained by excluding CC over the entire E_{trans} range. It has also been found that the dynamics is sensitive to the choice of K values considered in the calculation. Therefore, ideally, one needs to investigate the dynamics by including all the K values in the calculation. Unfortunately, with the limited computational facility available to us, this is not possible at present. However, efforts are under way to compute the integral reaction cross section by including all K values in a parallel computing environment.

Acknowledgment. A.K.T. thanks the Council of Scientific and Industrial Research (CSIR), New Delhi, for a research fellowship. This study was supported in part by a grant from CSIR, New Delhi. N.S. is an Honorary Professor at the Jawaharlal Nehru Centre for Advanced Scientific Research, Bangalore. N.S. thanks the Department of Science and Technology, New Delhi, for a J.C. Bose fellowship.

References and Notes

(1) Meijer, A. J. H. M.; Goldfield, E. M. *J. Chem. Phys.* **1999**, *110*, 870.
(2) Goldfield, E. M.; Meijer, A. J. H. M. *J. Chem. Phys.* **2000**, *113*, 11055.
(3) Padmanaban, R.; Mahapatra, S. *J. Phys. Chem. A* **2006**, *110*, 6039.
(4) Chu, T. S.; Lu, R. F.; Han, K. L.; Tang, X.-N.; Xu, H.-f.; Ng, C. Y. *J. Chem. Phys.* **2005**, *122*, 244322.
(5) Panda, A. N.; Sathyamurthy, N. *J. Chem. Phys.* **2004**, *121*, 9343.
(6) Palmieri, P.; Puzzarini, C.; Aquilanti, V.; Capecchi, G.; Cavalli, S.; De Fazio, D.; Aguilar, A.; Giménez, X.; Lucas, J. M. *Mol. Phys.* **2000**, *98*, 1835.
(7) Tang, X. N.; Xu, H.; Zhang, T.; Hou, Y.; Chang, C.; Ng, C. Y.; Chiu, Y.; Dressler, R. A.; Levandier, D. J. *J. Chem. Phys.* **2005**, *122*, 164301.
(8) Tiwari, A. K.; Panda, A. N.; Sathyamurthy, N. *J. Phys. Chem. A* **2006**, *110*, 389.
(9) Tiwari, A. K.; Sathyamurthy, N. *J. Phys. Chem. A* **2006**, *110*, 11200.
(10) Joseph, T.; Sathyamurthy, N. *J. Chem. Phys.* **1984**, *80*, 5332.
(11) Balakrishnan, N.; Kalyanaraman, C.; Sathyamurthy, N. *Phys. Rep.* **1997**, *280*, 79.
(12) Zhang, J. Z. H. *Theory and Applications of Quantum Molecular Dynamics*; World Scientific: Singapore, 1999.
(13) Gögtas, F.; Balint-Kurti, G. G.; Offer, A. R. *J. Chem. Phys.* **1996**, *104*, 7927.
(14) Marston, C. C.; Balint-Kurti, G. G. *J. Chem. Phys.* **1989**, *91*, 3571.
(15) Feit, M. D.; Fleck, J. A., Jr.; Steiger, A. *J. Chem. Phys.* **1982**, *47*, 412.
(16) Kosloff, D.; Kosloff, R. *J. Comput. Phys.* **1983**, *52*, 35.
(17) Parker, G. A.; Light, J. C. *Chem. Phys. Lett.* **1982**, *89*, 483. Light, J. C.; Hamilton, I. P.; Lill, J. V. *J. Chem. Phys.* **1985**, *82*, 1400.
(18) Quéré, F.; Leforestier, C. *J. Chem. Phys.* **1990**, *92*, 247. Leforestier, C. *J. Chem. Phys.* **1990**, *94*, 6388.
(19) Corey, G. C.; Lemoine, D. *J. Chem. Phys. D* **1992**, *97*, 4115.
(20) Kalyanaraman, C.; Clary, D. C.; Sathyamurthy, N. *J. Chem. Phys.* **1999**, *111*, 10910.
(21) Maiti, B.; Kalyanaraman, C.; Panda, A. N.; Sathyamurthy, N. *J. Chem. Phys.* **2002**, *117*, 9719.
(22) Tiwari, A. K.; Sathyamurthy, N. *Chem. Phys. Lett.* **2005**, *414*, 509.
(23) Turner, T.; Dutuit, O.; Lee, Y. T. *J. Chem. Phys.* **1984**, *81*, 3475.
(24) Tang, X. N.; Houchins, C.; Xu, H. F.; Ng, C. Y.; Chiu, Y.; Dressler, R. A.; Levandier, D. J. *J. Chem. Phys.* **2007**, *126*, 234305.
(25) Tang, X.; Houchins, C.; Lau, K. C.; Ng, C. Y.; Dressler, R. A.; Chiu, Y. H.; Chu, T. S.; Han, K. L. *J. Chem. Phys.* **2007**, *127*, 164318.

JP9049523